Age-Related Distribution of the Copper-Beaten Skull Appearance on Pediatric Cephalometric Radiographs: A Retrospective Single-Center Study

Thomas Saliba[1*], Alessandro De Leucio[1], Paolo Simoni[1], Grammatina Boitsios[1]

[1] Hôpital des Enfants Reine Fabiola, Brussels, Belgium

ORCID: Thomas Saliba 0000-0001-6989-9577 | Alessandro De Leucio 0000-0001-6180-1483 | Paolo Simoni 0000-0002-5957-0644 | Grammatina Boitsios 0000-0003-1575-9119

Swiss Journal of Radiology and Nuclear Medicine - SJORANM GmbH - Rosenweg 3 - CH-6340 Baar - Switzerland

Abstract

Background: The copper-beaten skull (CBS) appearance on lateral skull radiographs has historically been associated with raised intracranial pressure, but convolutional markings may also occur during normal cranial development. We aimed to characterize the age-related distribution of CBS in a contemporary pediatric orthodontic referral cohort and to compare the observed pattern with classic historical series.

Methods: This single-center retrospective study included 748 lateral skull radiographs from unique patients aged 3–19 years obtained for orthodontic indications between July 2008 and April 2023 (378 female, 370 male). Radiographs were graded 0–3 by two blinded radiologists, with disagreements resolved by consensus. Because the outcome was ordinal and the contingency table contained sparse cells, analyses included a Monte Carlo permutation test, Spearman and Kendall rank correlations, proportional-odds ordinal logistic regression with age, quadratic age, sex, age-by-sex interaction, and sampling period, plus bootstrap and threshold-specific robustness analyses.

Results: Grade distribution was grade 0, n = 55 (7.4%); grade 1, n = 162 (21.7%); grade 2, n = 444 (59.4%); and grade 3, n = 87 (11.6%). Monte Carlo testing confirmed an age–grade association ($p = .00055$), although rank correlations were weak (Spearman's $\rho = -0.149$; Kendall's τ-b = −0.115; both $p < .001$). The ordinal model showed a significant nonlinear age effect (linear OR = 0.913, 95% CI 0.858–0.971, $p = .004$; quadratic OR = 0.977, 95% CI 0.964–0.991, $p = .001$). Sex, age-by-sex interaction, and sampling period were not significant. Results were directionally similar in the date-restricted principal-period sensitivity cohort (n = 554).

Conclusion: Convolutional skull markings were common in this pediatric orthodontic referral cohort and varied with age but not significantly with sex. A copper-beaten skull appearance should not be interpreted in isolation as evidence of raised intracranial pressure. Because the cohort was selectively supplemented by age and participants were not systematically screened for neurological or craniofacial disease, the observed frequency is not a population prevalence estimate and does not establish physiological normality.

Keywords: Copper-beaten skull; cephalometric radiograph; skull; intracranial pressure; pediatric radiology; convolutional markings

**Corresponding author: Dr Thomas Saliba, Hôpital des Enfants Reine Fabiola, Route de Lennik 808, 1070 Bruxelles, Belgium.* *Tel. +32 (0)2 477 31 69*; *Email:* Tes1066@hotmail.com

Presented as an abstract at the ESSR Congress, Bilbao, 2023. Submitted 17.07.2026. Peer reviewed and accepted 13.08.2026.

Introduction

The copper-beaten skull (CBS) appearance refers to prominent convolutional impressions of the inner table visible on conventional skull radiographs (Sharma et al., 2014). Historically, this appearance was associated with raised intracranial pressure in conditions such as intracranial masses, hydrocephalus, and craniosynostosis, although developmental explanations were proposed early in the radiological literature (du Boulay, 1956; Ginelliová et al., 2016; Macaulay, 1951; Sharma et al., 2014). Subsequent observations have shown that CBS is neither sensitive nor specific for raised intracranial pressure or craniosynostosis and therefore cannot be interpreted as an isolated diagnostic sign (du Boulay, 1956; Macaulay, 1951; Sharma et al., 2014).

Convolutional impressions are thought to reflect the interaction between the growing brain and the still-malleable inner table of the pediatric skull. They have been described as particularly conspicuous during periods of rapid brain growth, including approximately ages 2–3 and 5–7 years, and are expected to diminish with increasing cranial maturity (Mahomed et al., 2012; Sharma et al., 2014). The underlying morphology corresponds to impressions produced by the cerebral gyri and sulci, and the markings generally become less prominent around puberty unless additional factors, including persistently raised intracranial pressure, are present (Mahomed et al., 2012; Sharma et al., 2014).

A pronounced CBS appearance may nevertheless occur in association with pathological cranial development, particularly craniosynostosis syndromes such as Crouzon, Pfeiffer, and Apert syndromes (Ginelliová et al., 2016; Mahomed et al., 2012; Phore & Panchal, 2018). The clinical relevance of the sign therefore depends on age, distribution, associated radiographic abnormalities, and the broader clinical context.

The aim of this study was to characterize the age-related distribution of CBS in a contemporary pediatric orthodontic referral cohort and to compare the observed pattern with the classic studies of Davidoff, Macaulay, and du Boulay (Davidoff, 1936; Macaulay, 1951; du Boulay, 1956). We specifically examined whether grade distribution varied with age or sex. Because the cohort was not systematically screened for neurological or craniofacial disease, the study was not designed to establish physiological normality, population prevalence, or diagnostic accuracy.

Materials and Methods

Study population and PACS search strategy

This single-center retrospective study was conducted at the Hôpital Universitaire des Enfants Reine Fabiola (HUDERF), Brussels, Belgium, and was approved by the local ethics committee (CEH no. 38/23); informed consent was waived. Eligible examinations were lateral skull radiographs obtained for orthodontic care in patients aged 0–19 years. Examinations performed for non-orthodontic indications and examinations of patients older than 19 years were not eligible. Known intracranial hypertension, known craniofacial or skull deformity, and absence of an associated image were additional exclusion criteria.

We searched the institutional picture archiving and communication system (PACS) for lateral skull radiographs obtained for orthodontic care using the examination filter "télécrane" (Table 1). The initial search was intended to cover the principal sampling period from 1 October 2013 to 26 April 2023 and yielded 513 radiographs. In practice, the examinations returned by this query were dated from 24 November 2017 onward. Because the age distribution was strongly concentrated between 10 and 15 years, two supplementary, non-date-restricted PACS searches were performed to enrich the older-adolescent and younger-child age groups; these returned 120 and 130 additional radiographs, respectively. For the purposes of this retrospective cohort description, the supplementary search labels "15–19 years" and "6–9 years" are used as target-group labels for the PACS enrichment strategy rather than as strict retrospective age-at-examination boundaries for every record ultimately recovered. The earliest examination in the final dataset was dated 10 July 2008. Hospital patient numbers were used to verify that each examination represented a unique child and that records returned by more than one search were counted only once. Of 763 identified examinations, 15 were excluded (4 without an associated image, 2 with known intracranial hypertension, and 9 with known craniofacial or skull deformity), leaving 748 examinations for analysis (Figure 1; Table 8). Of these, 554 were performed within the principal sampling period and 194 before 1 October 2013. The initial search contributed 502 included examinations (513 identified minus 11 exclusions), while the supplementary searches contributed a further 52 included examinations within the principal period, giving 554 in-period examinations in total. Thirty-five of these 52 examinations involved patients who were aged 15–18 years at the time of examination but were already older than 19 years (aged 20–27 years) at the date of the initial PACS query and were therefore recovered only by the supplementary search. The remaining 17 in-period examinations involved children aged 3–7 years at the time of examination and were also recovered by the supplementary searches; these examinations were dated between 15 November 2013 and 7 August 2017, before the effective retrieval window of the initial query, and the children were aged 10–17 years at the date of the query. No attempt was made to balance the sex distribution. Age and sex distributions are shown in Figures 2 and 3.

Radiographic acquisition

Digital radiographs were acquired in a lateral projection with the patient positioned side-on to the x-ray tube at an approximate source-to-patient distance of 100 cm. Tube voltage and exposure were adapted to the individual patient. Images were reviewed on PACS workstations using the vendor display settings, and no additional post-processing was applied for grading. Diagnostic image adequacy was assessed by both readers during grading; examinations without an associated image were excluded, and none of the available images was considered non-diagnostic. Detailed retrospective information on the radiography system manufacturer/model and on possible equipment or protocol changes across the study period was not available for this analysis.

Patient age was defined as age at the date of examination.

Image grading

The radiographs were independently reviewed by two radiologists: one resident with two years of experience (TS) and one consultant neuroradiologist with more than ten years of experience (GB). Readers used the standardized four-point grading system described by du Boulay and derived from Macaulay (du Boulay, 1956; Macaulay, 1951). Disagreements were resolved by consensus, and only the final consensus grade was retained.

Classification

- Grade 0: no visible copper-beaten appearance.
- Grade 1: few, shallow convolutional markings.
- Grade 2: moderate convolutional markings.
- Grade 3: deep and extensive convolutional impressions.

An example of a typical skull for each classification is depicted in Figure 4.

Both readers were blinded to patient age, sex, and medical history during image grading.

After grading, available medical records were reviewed for relevant clinical information, with particular attention to documented intracranial hypertension and craniofacial abnormalities. Most patients had no longitudinal clinical follow-up at the institution beyond the radiographic examination, so clinical-history data were unavailable for the majority of the cohort. Consequently, pre-existing neurological or craniofacial disease cannot be excluded in patients without documented histories. Patients with known intracranial hypertension or known craniofacial/skull deformity identified in the available records were excluded before analysis.

Statistical analysis

CBS grade was summarized by age and sex in a contingency table (Table 3) and displayed graphically (Figures 5 and 6). Because CBS grade is ordinal (0–3) and the age–grade relationship was expected to be nonlinear, analysis extended beyond a conventional chi-square test. We first assessed the single-year age × grade table for chi-square adequacy, then used a Monte Carlo permutation test (20,000 resamples) and rank-based measures of ordinal association (Spearman's ρ and Kendall's τ-b) (Table 4). A proportional-odds ordinal logistic regression model was fitted with CBS grade as the outcome and age (mean-centered, with a quadratic term), sex, age × sex interaction, and sampling period (before vs. on/after October 2013) as covariates (Table 5). Model-based Wald 95% confidence intervals were cross-checked with a 400-replicate case-resampling bootstrap (Table 6). The proportional-odds assumption was assessed with a Brant test; because this test indicated departure from strict proportional odds, age effects were also estimated in threshold-specific binary logistic regressions for grade ≥1, grade ≥2, and grade ≥3. A sensitivity analysis repeated the principal analyses in the date-restricted principal-period cohort (n = 554; Table 2). Descriptive age-group medians and interquartile ranges were summarized in Table 7; median 95% confidence intervals were estimated using a 2,000-replicate bootstrap within each age group, except for groups with n = 1, for which the interval was not estimable. All 748 included examinations represented unique patients, so no clustering adjustment was required. Analyses were performed in Python using statsmodels 0.14 and scipy 1.17. The analysis script was generated with assistance from Claude Sonnet 5 (Anthropic, California, USA) and was manually checked before execution.

Results

Clinical-history information was sparse because most patients were not followed longitudinally at HUDERF after the orthodontic radiograph. Among patients with available records, only a small number had documented intracranial hypertension, and these cases were excluded from the analytical cohort. Because the available clinical metadata were incomplete, analyses were limited to age, sex, sampling period, and CBS grade.

Cohort characteristics and age–grade association

Seven hundred and forty-eight unique patients were analyzed. The single-year age (17 levels) × grade (4 levels) table comprised 68 cells (df = 48), of which 28 (41%) had expected counts below 5. The standard chi-square approximation was therefore considered unreliable despite a nominally significant result ($\chi^2 = 93.21$, df = 48, $p < .001$). A Monte Carlo permutation test (20,000 resamples), which does not depend on the same asymptotic assumptions, confirmed an age–grade association (p = .00055). Rank-based analyses showed only a weak inverse association between age and grade (Spearman's ρ = −0.149, 95% bootstrap CI −0.223 to −0.074, $p < .001$; Kendall's τ-b = −0.115, 95% CI −0.171 to −0.058, $p < .001$).

Ordinal regression and sensitivity analysis

In the proportional-odds model, age showed a significant nonlinear association with CBS grade. Both the linear age term (OR = 0.913 per year at the mean age, 95% CI 0.858–0.971, p = .004) and the quadratic term (OR = 0.977, 95% CI 0.964–0.991, p = .001) were significant, consistent with higher grades at intermediate ages and lower grades toward the youngest and oldest ends of the sampled age range. Sex was not significantly associated with grade (OR = 0.864, 95% CI 0.651–1.147, p = .312), and the age × sex interaction was not significant (OR = 0.993, 95% CI 0.910–1.083, p = .873). Sampling period was also not significant (OR = 0.788, 95% CI 0.548–1.134, p = .199). The Brant test indicated a modest departure from strict proportional odds ($\chi^2(8) = 17.50$, p = .025), driven mainly by the youngest age groups. Threshold-specific binary logistic regressions nevertheless estimated age ORs below 1 at each threshold (grade ≥1: OR 0.802, 95% CI 0.687–0.937; grade ≥2: OR 0.909, 95% CI 0.847–0.975; grade ≥3: OR 0.948, 95% CI 0.854–1.052). Bootstrap confidence intervals were consistent with the model-based estimates for all covariates.

To assess the influence of the supplementary non-date-restricted searches, the analyses were repeated in the 554 examinations obtained within the principal sampling period (1 October 2013–26 April 2023), excluding the 194 examinations performed before 1 October 2013 (Table 2). Grade distribution was similar to that of the full cohort (grade 0/1/2/3: 7.8%/20.9%/60.3%/11.0% vs. 7.4%/21.7%/59.4%/11.6%). The age–grade association remained significant by Monte Carlo testing (p = .00035), with rank correlations similar to the full cohort (Spearman's ρ = −0.145; Kendall's τ-b = −0.117). In the reduced ordinal model, the linear age term remained directionally similar but was not statistically significant (OR = 0.934, 95% CI 0.860–1.016, p = .111), and the quadratic term was borderline (OR = 0.983, 95% CI 0.967–1.000, $p = .051$). Sex and the age × sex interaction remained non-significant. The Brant test again indicated departure from strict proportional odds ($\chi^2(8) = 15.91$, $p = .044$). Overall, the sensitivity analysis did not suggest a qualitative change in the direction of the age–grade relationship, although estimates were less precise in the smaller date-restricted cohort.

Discussion

Davidoff's 1936 series of 2,500 cranial radiographs was among the earliest systematic descriptions of age-related convolutional markings. He reported few markings in infancy, increasing prominence during early childhood, a plateau through much of childhood, and subsequent decline with increasing age (Davidoff, 1936; du Boulay, 1956). These observations helped establish the concept that convolutional markings can accompany normal cranial growth rather than invariably indicating pathological intracranial pressure.

Macaulay subsequently reviewed 296 pediatric skull radiographs and likewise observed increasing visibility during the first years of life, a relatively stable pattern from approximately 4 to 10 years, and later decline. In the 4–10-year age range, most children showed at least some convolutional markings, whereas only a minority had particularly prominent impressions (Macaulay, 1951).

The age-related pattern in the present cohort broadly parallels these historical observations. Grades were most consistently prominent between approximately 6 and 13 years and tended to decline during later adolescence. The association with age was statistically significant but weak in rank-based analyses and clearly nonlinear in the ordinal regression model. No significant sex effect or age-by-sex interaction was demonstrated. The very small numbers at ages 3–5 years and at age 19 should be considered when interpreting the extremes of the age distribution.

Du Boulay compared children with and without raised intracranial pressure and emphasized that convolutional markings were more informative when persistent, pronounced, and interpreted together with other radiographic and clinical signs. In his series, suture diastasis and changes involving the sella turcica could precede or accompany increased convolutional markings, while marked gyral impressions were also observed in children without recognized pathology (du Boulay, 1956). This historical work therefore already argued against treating CBS as a stand-alone sign.

Van der Meulen et al. examined the beaten-copper pattern in children with craniosynostosis and found no association between the radiographic appearance and later intelligence quotient in their operated cohort. They also noted that, after early childhood, the frequency of the pattern overlapped substantially with historical observations in children without craniosynostosis (Van Der Meulen et al., 2008).

Taken together, the current and historical evidence indicates that CBS is neither sufficiently sensitive nor sufficiently specific to diagnose raised intracranial pressure in isolation. Associated findings, including cranial suture diastasis and other manifestations of altered cranial growth, as well as the clinical presentation, remain essential to interpretation (Sharma et al., 2014; Van Der Meulen et al., 2008). The high frequency of convolutional markings in this orthodontic referral cohort confirms that the finding is common during childhood, but it does not establish physiological normality.

This study has several limitations. First, the supplementary age-targeted PACS searches created a non-uniform sampling strategy. Although sampling period was included as a covariate and a date-restricted sensitivity analysis was performed, selection bias cannot be excluded. Second, clinical-history and follow-up information were unavailable for most patients, limiting the ability to rule out unrecorded neurological or craniofacial disease. Third, only the final consensus grade was archived; reader-specific scores were not retained, so interobserver agreement and reproducibility of the grading system could not be quantified. Fourth, detailed information on the radiographic equipment and any changes in acquisition protocols across the long study period was not available, and differences in equipment, image processing, or image quality could have influenced the visibility of convolutional markings. Finally, direct comparison with historical series is limited by differences in study populations, equipment, clinical information, grading methods, reader experience, and image quality.

Conclusion

Convolutional skull markings were frequently observed on lateral cephalometric radiographs in this pediatric orthodontic referral cohort, with grade distribution varying by age but not significantly by sex. A copper-beaten skull appearance should not, in isolation, be considered evidence of raised intracranial pressure; clinical presentation and associated imaging findings remain essential. Because the cohort was selectively supplemented by age and was not systematically assessed for neurological or craniofacial disease, the observed frequency should not be interpreted as a population prevalence estimate, a diagnostic accuracy measure, or definitive proof of physiological normality.

References

1. Sharma R, Priyadarshinni SR, Desai V. Copper Beaten Skull! Can It be a Usual Appearance? International Journal of Clinical Pediatric Dentistry. 2014;7(1):47. https://doi.org/10.5005/JP-JOURNALS-10005-1233.
2. Ginelliová A, Farkaš D, Iannaccone SF, Vyhnálková V, Vasovčák P. Sudden death associated with syndromic craniosynostosis. Forensic Science, Medicine, and Pathology. 2016;12(4):506–509. https://doi.org/10.1007/S12024-016-9818-5.
3. du Boulay G. The Significance of Digital Impressions in Children's Skulls. Acta Radiologica. 1956;46(1–2):112–122. https://doi.org/10.1177/028418515604600116.
4. Macaulay D. Digital markings in radiographs of the skull in children. British Journal of Radiology. 1951;24(288):647–652. https://doi.org/10.1259/0007-1285-24-288-647.
5. Mahomed N, Sewchuran F. The copper-beaten skull. South African Journal of Radiology. 2012;16(1):25–26. https://doi.org/10.4102/SAJR.V16I1.229.
6. Phore S, Panchal R. Beaten silver appearance: Normal or pathognomic in children? International Journal of Oral Health Sciences. 2018;8(1):51. https://doi.org/10.4103/ijohs.ijohs_28_17.
7. Davidoff L. Convolutional digitations seen in the roentgenograms of immature human skulls. Bull Neurol Inst NY. 1936;5:61–71.
8. Van Der Meulen J, Van Der Vlugt J, Okkerse J, Hofman B. Early beaten-copper pattern: its long-term effect on intelligence quotients in 95 children with craniosynostosis. Journal of Neurosurgery: Pediatrics. 2008;1(1):25–30. https://doi.org/10.3171/PED-08/01/025.

Declarations

Ethics approval

The study was approved by the local ethics committee of the Hôpital Universitaire des Enfants Reine Fabiola (CEH no. 38/23); informed consent was waived.

Funding

No funding was received for this work.

Conflicts of interest

None of the authors have any conflicts of interest to report.

Data availability

The anonymized analytical dataset and the statistical analysis code used in this study are available from the corresponding author upon reasonable request. The original radiographs are not shared because they constitute identifiable patient data subject to the data-protection rules of the Hôpital Universitaire des Enfants Reine Fabiola.

Correspondence to

Dr Thomas Saliba
Hôpital des Enfants Reine Fabiola
Route de Lennik 808, 1070 Bruxelles, Belgium
Tes1066@hotmail.com
ORCID: 0000-0001-6989-9577

Disclaimer/Publisher's Note

License Policy

Figures

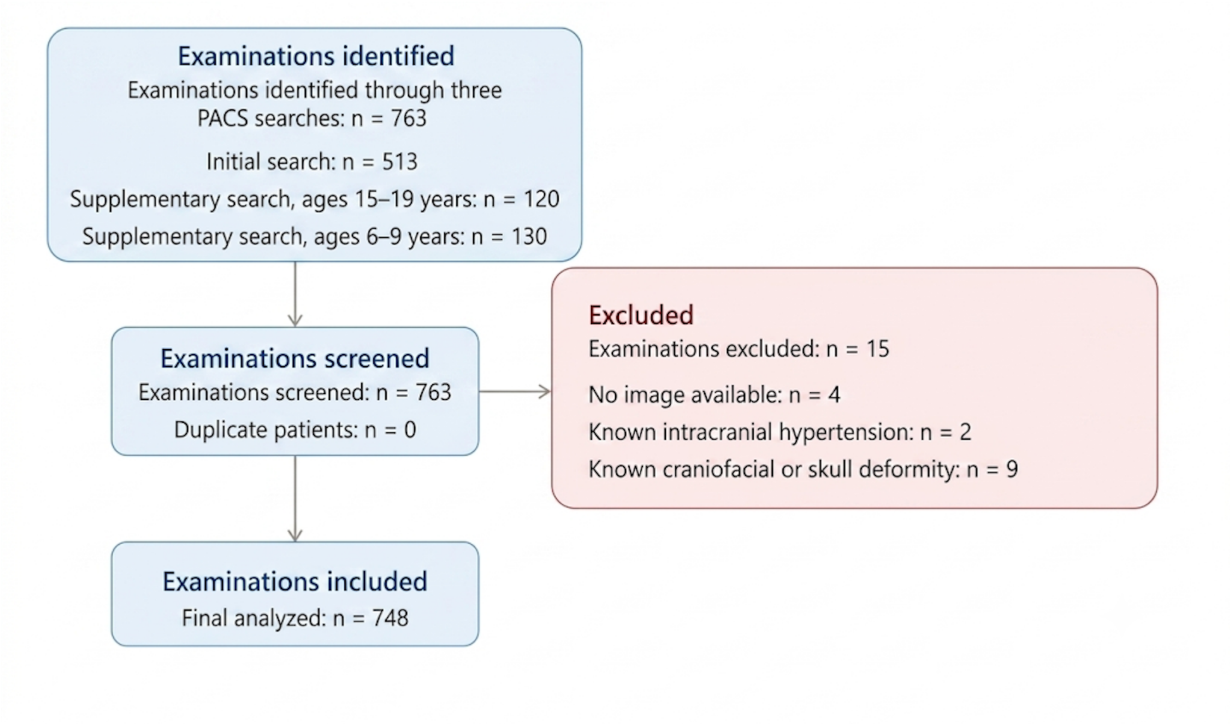

Fig. 1. Flowchart of the patient inclusion process. Supplementary age labels indicate target groups for cohort enrichment rather than strict retrospective age-at-examination boundaries.

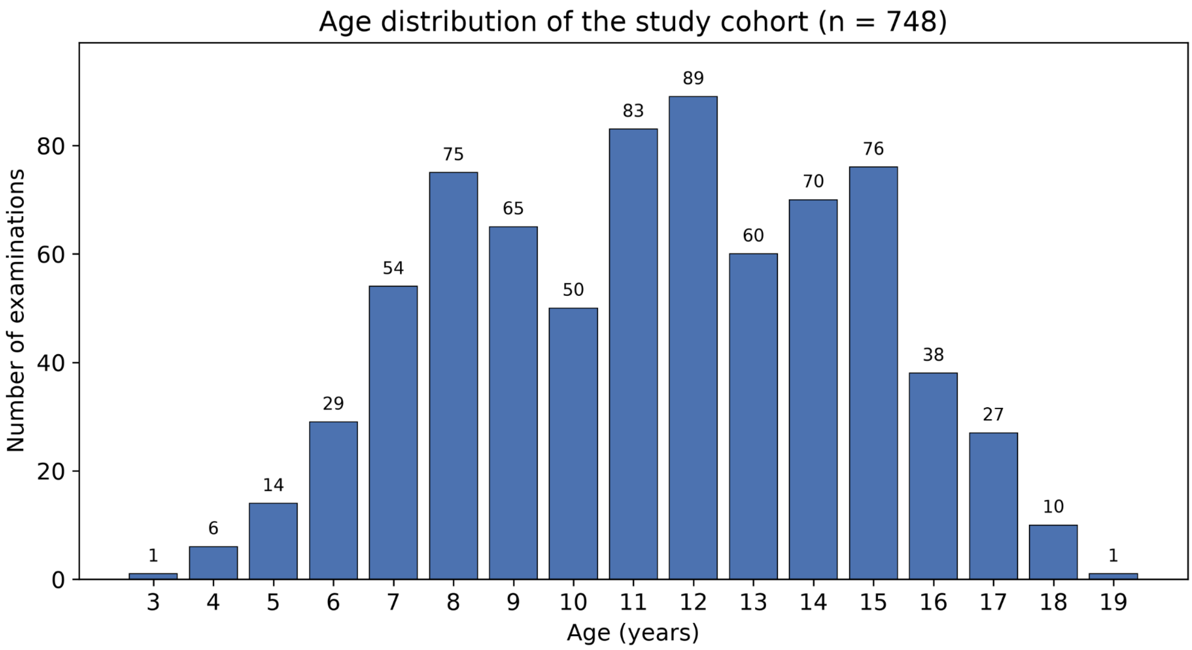

Fig. 2. Age distribution of the study cohort

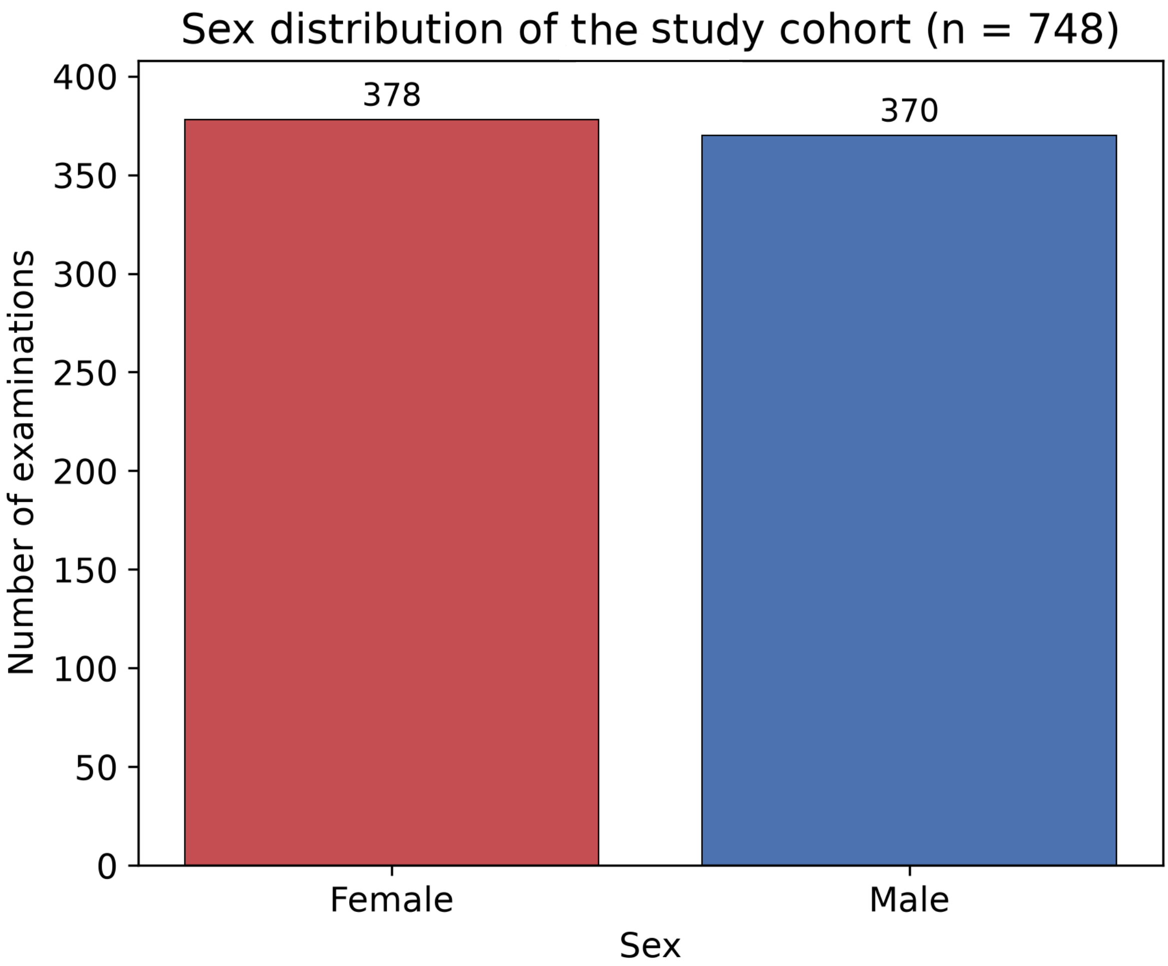

Fig. 3. Sex distribution of the study cohort

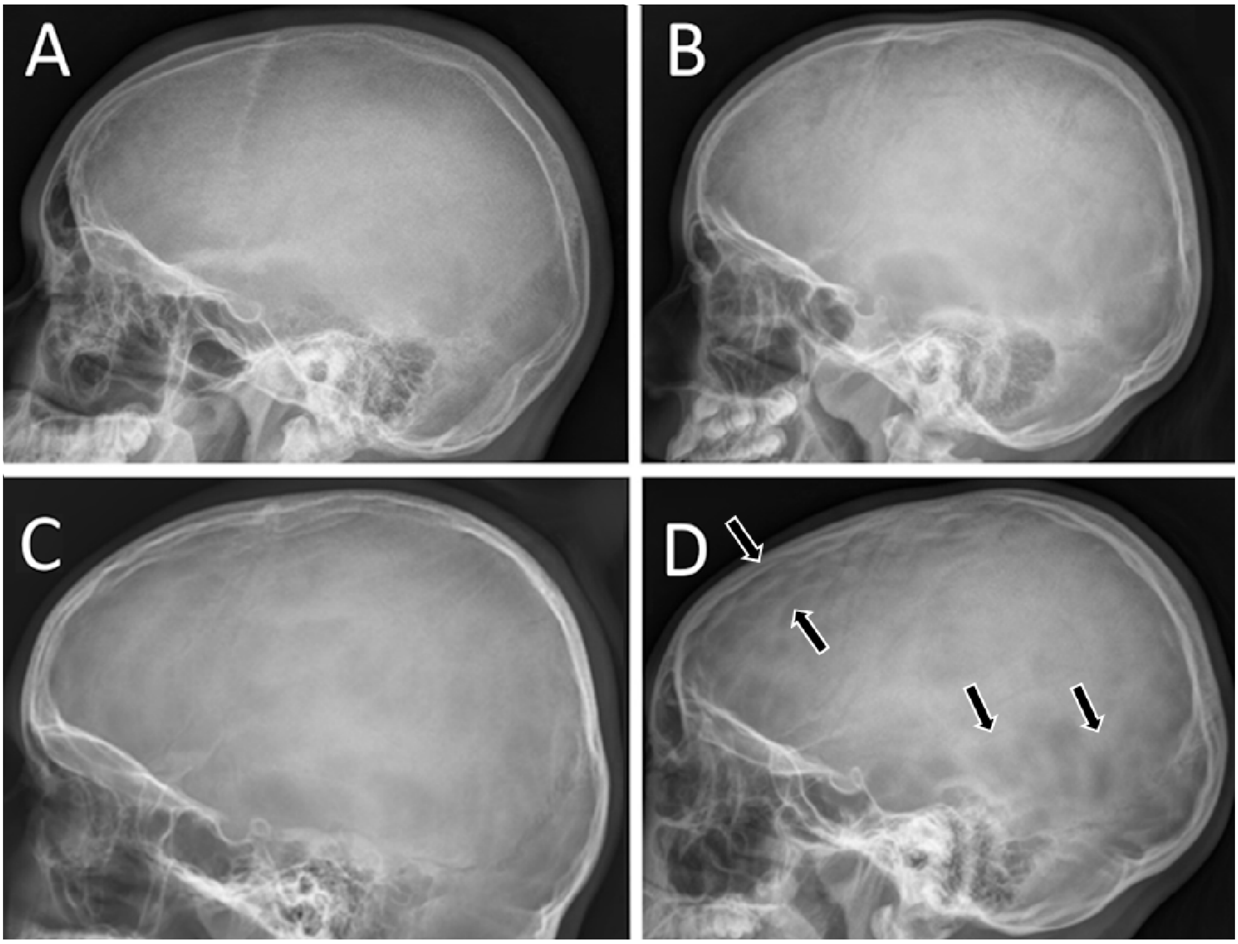

Fig. 4. Representative examples of copper-beaten skull grades 0–3 on lateral cephalometric radiographs. A: Grade 0, no visible convolutional markings. B: Grade 1, few and shallow convolutional markings. C: Grade 2, moderate convolutional markings. D: Grade 3, extensive and prominent convolutional markings, indicated by arrows.

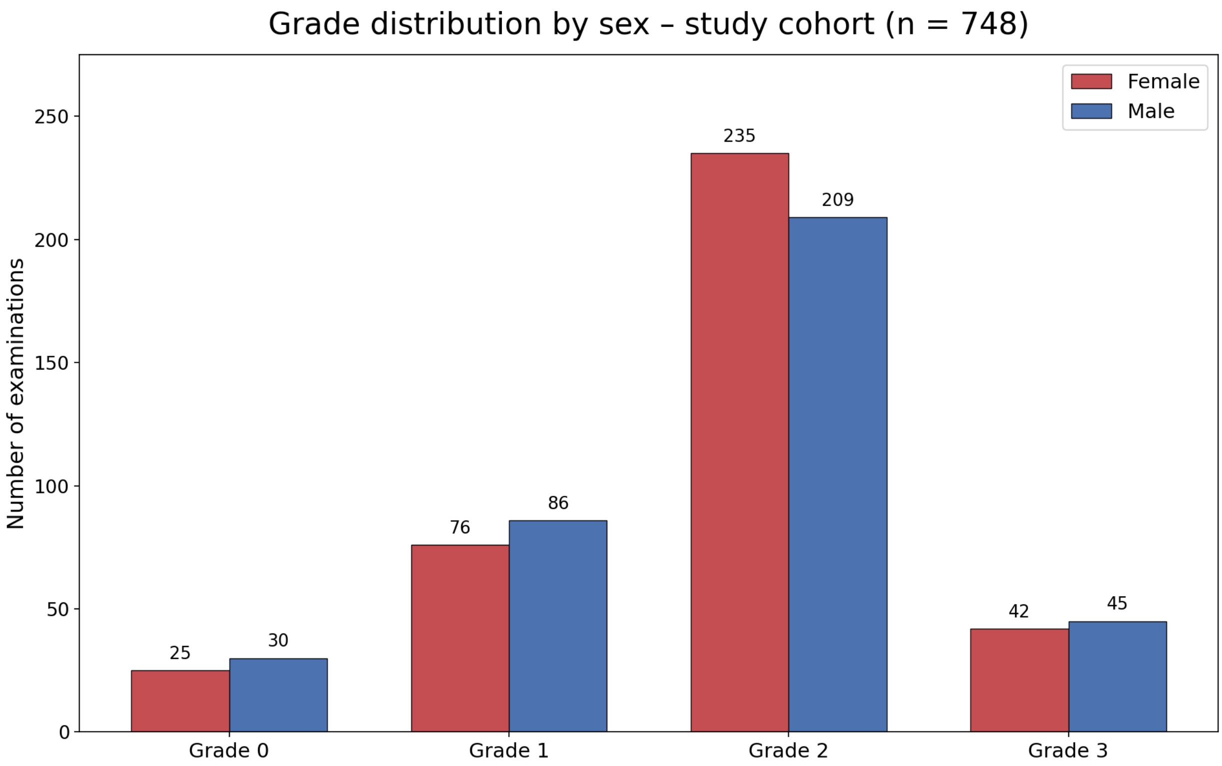

Fig. 5. Distribution of copper-beaten skull grades according to sex. Bars show the number of examinations assigned to grades 0, 1, 2, and 3 among female and male patients.

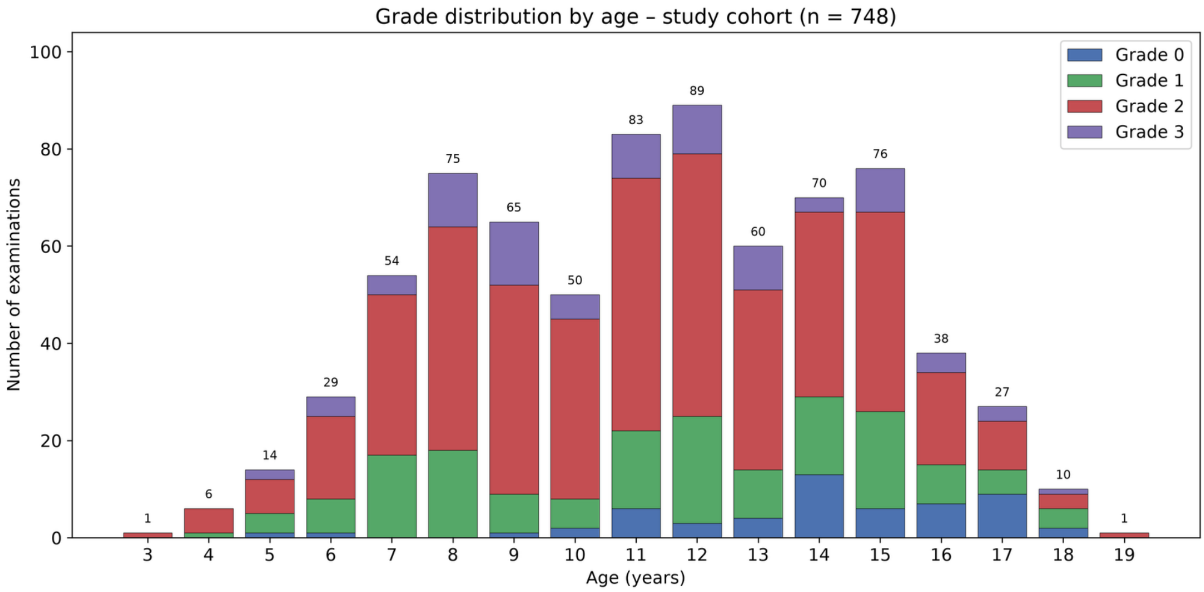

Fig. 6. Distribution of copper-beaten skull grades by age. Stacked bars show the number of examinations assigned to grades 0–3 at each completed year of age. The total number of examinations in each age group is displayed above the corresponding bar.

Tables

Table 1

PACS search strategy and yield of the three queries. Duplicate examinations across searches (verified by hospital patient number) were counted once; no duplicates were identified. The age labels of the two supplementary searches denote the intended target groups used for cohort enrichment and are not treated here as strict retrospective age-at-examination boundaries for every retrieved record. Exclusion reasons are detailed in Table 8.

Search	Date range	Age range	Search term / filter	Identified (n)	Excluded (n)	Included (n)
1. Initial	24 Nov 2017 – 26 Apr 2023 (examinations retrieved)	0–19 years (at time of query)	“Télécrane” (lateral skull, orthodontic)	513	11	502
2. Older-age search	No date restriction (earliest: 10 Jul 2008)	Target group: 15–19 years	“Télécrane”	120	1	119
3. Younger-age search	No date restriction	Target group: 6–9 years	“Télécrane”	130	3	127
Total	10 Jul 2008 – 26 Apr 2023	3–19 years (observed)		763	15	748

Table 2

Comparison of the full cohort with the date-restricted principal-period sensitivity cohort (1 October 2013–26 April 2023). The sensitivity ordinal model used the same specification as the primary model (age mean-centered at the full-cohort mean with a quadratic term, sex, and age × sex); the sampling-period covariate was omitted because it is constant within the principal period. Confidence intervals are Wald 95% confidence intervals.

Statistic	Full cohort (n = 748)	Date-restricted principal-period cohort (n = 554)
Grade distribution (0/1/2/3)	55/162/444/87 (7.4%/21.7%/59.4%/11.6%)	43/116/334/61 (7.8%/20.9%/60.3%/11.0%)
Monte Carlo permutation p-value (20,000 resamples)	.00055	.00035
Spearman’s ρ (95% CI)	−0.149 (−0.223 to −0.074), p < .001	−0.145 (−0.229 to −0.059), p < .001
Kendall’s τ-b (95% CI)	−0.115 (−0.171 to −0.058), p < .001	−0.117 (−0.186 to −0.047), p < .001
Age, linear (OR per year at mean age)	0.913 (0.858–0.971), p = .004	0.934 (0.860–1.016), p = .111
Age, quadratic (OR)	0.977 (0.964–0.991), p = .001	0.983 (0.967–1.000), p = .051
Sex, male vs. female (OR)	0.864 (0.651–1.147), p = .312	0.980 (0.703–1.367), p = .905
Age × sex interaction (OR)	0.993 (0.910–1.083), p = .873	0.914 (0.810–1.031), p = .143
Sampling period (≥1 Oct 2013 vs. before) (OR)	0.788 (0.548–1.134), p = .199	n/a – constant within the principal period
Brant test (proportional odds)	$\chi^2(8)$ = 17.50, p = .025	$\chi^2(8)$ = 15.91, p = .044

Table 3

Contingency table of the copper-beaten skull grades by age and by sex.

e (years)	Sex	Grade 0	Grade 1	Grade 2	Grade 3	Total	Percentage
	Male	0	0	1	0	1	0.13
	Female	0	1	2	0	3	0.40
	Male	0	0	3	0	3	0.40
	Female	0	1	4	1	6	0.80
	Male	1	3	3	1	8	1.07
	Female	0	0	9	3	12	1.60
	Male	1	7	8	1	17	2.27
	Female	0	9	16	2	27	3.61
	Male	0	8	17	2	27	3.61
	Female	0	8	28	6	42	5.61
	Male	0	10	18	5	33	4.41
	Female	1	3	21	7	32	4.28
	Male	0	5	22	6	33	4.41
	Female	1	4	21	1	27	3.61
	Male	1	2	16	4	23	3.07
	Female	5	8	29	3	45	6.02
	Male	1	8	23	6	38	5.08
	Female	2	11	29	4	46	6.15
	Male	1	11	25	6	43	5.75
	Female	2	6	17	3	28	3.74
	Male	2	4	20	6	32	4.28
	Female	6	7	17	2	32	4.28
	Male	7	9	21	1	38	5.08
	Female	4	7	22	9	42	5.61
	Male	2	13	19	0	34	4.55
	Female	3	6	10	1	20	2.67
	Male	4	2	9	3	18	2.41
	Female	0	2	7	0	9	1.20

e (years)	Sex	Grade 0	Grade 1	Grade 2	Grade 3	Total	Percentage
	Male	9	3	3	3	18	2.41
	Female	1	3	2	0	6	0.80
	Male	1	1	1	1	4	0.53
	Female	0	0	1	0	1	0.13
al	-	55	162	444	87	748	100
centage	-	7.35	21.66	59.36	11.63	100.00	-

Table 4

Overview of the statistical tests performed.

Statistic	Value
Table dimensions	17 age groups × 4 grades (68 cells)
Degrees of freedom	48
Chi-square statistic	93.21
Chi-square p-value	< .001 (p = .0001)
Cells with expected count < 5	28 / 68 (41%)
Cramér's V (bias-corrected)	0.142
Monte Carlo permutation p-value (20,000 resamples)	.00055
Spearman's ρ (age, grade)	−0.149 (95% CI −0.223 to −0.074), p < .001
Kendall's τ-b (age, grade)	−0.115 (95% CI −0.171 to −0.058), p < .001

Table 5

Ordinal logistic regression table. Proportional-odds model. Outcome: CBS grade (0–3), n = 748. Age is mean-centered (age c) with a quadratic term (age c²). The threshold parameters separate the four ordered grade categories and are not covariate effects.

Parameter	Coef.	SE	z	p	95% CI
Age, centered (age c)	−0.091	0.032	−2.877	.004	−0.153 to −0.029
Age, centered² (age c²)	−0.023	0.007	−3.323	.001	−0.036 to −0.009
Sex (male vs. female)	−0.146	0.145	−1.010	.312	−0.429 to 0.137
Age × sex interaction	−0.007	0.044	−0.160	.873	−0.094 to 0.080
Period (≥1 Oct 2013 vs. before)	−0.238	0.186	−1.283	.199	−0.602 to 0.126
Threshold 0/1	−3.083	0.250	−12.321	< .001	−3.573 to −2.592
Threshold 1/2	0.524	0.077	6.792	< .001	0.373 to 0.675
Threshold 2/3	1.095	0.042	25.804	< .001	1.012 to 1.178

Model fit: log-likelihood = −795.74; AIC = 1607; BIC = 1644; 748 observations, 5 covariate df.

Table 6

Odds ratio table with Wald and bootstrap confidence intervals.

Covariate	OR	Wald 95% CI	Bootstrap 95% CI	p-value
Age (centered, linear)	0.913	0.858–0.971	0.855–0.965	.004
Age (centered, quadratic)	0.977	0.964–0.991	0.964–0.989	.001
Sex (male vs. female)	0.864	0.651–1.147	0.653–1.151	.312
Age × sex interaction	0.993	0.910–1.083	0.902–1.089	.873
Period (≥1 Oct 2013 vs. before)	0.788	0.548–1.134	0.533–1.117	.199

Bootstrap: 400-replicate independent-case resampling (all 400 replicates converged).

Table 7

Grade distribution by age. Median 95% CI from a 2,000-replicate bootstrap within each age group; this was not estimable for the n = 1 groups (ages 3 and 19).

Age (years)	n	Median	IQR (Q1–Q3)	Median 95% CI
3	1	2	2–2	—
4	6	2	2–2	1.5–2.0
5	14	2	1–2	1.0–2.0
6	29	2	1–2	2.0–2.0
7	54	2	1–2	2.0–2.0
8	75	2	2–2	2.0–2.0
9	65	2	2–2	2.0–2.0
10	50	2	2–2	2.0–2.0
11	83	2	1–2	2.0–2.0
12	89	2	1–2	2.0–2.0
13	60	2	2–2	2.0–2.0
14	70	2	1–2	1.0–2.0
15	76	2	1–2	2.0–2.0
16	38	2	1–2	1.0–2.0
17	27	1	0–2	0.0–2.0
18	10	1	1–2	0.5–2.0
19	1	2	2–2	—

Table 8

Excluded patients by age and reason for exclusion.

Age	n excluded	Reasons
6y	1	Cranial deformity
7y	2	Cranial deformity
8y	2	No image
9y	1	Known intracranial hypertension
10y	2	Cranial deformity
11y	1	No image
12y	1	Cranial deformity
14y	4	1 no image, 1 known ICH, 2 cranial deformity
18y	1	Cranial deformity